Lion Optimization Algorithm for Load Frequency Control of Multi-Area Interconnected Power Systems with FACTS

M. Rajkumar[*1], Dr. S. Padma[2], Dr. R. Kannan[3]

[*1]*Research Scholar, Department of Electrical Engineering, Annamalai University, Annamalainagar, Tamil Nadu, India.*
[2,3]*Associate Professor, Department of Electrical Engineering, Annamalai University, Annamalainagar, Tamil Nadu, India*

KEYWORDS
Load Frequency Control (LFC); Multi-area power system; Proportional-Integral (PI) controller; Lion Optimization Algorithm (LOA).

ABSTRACT:
This work introduces the Lion Optimization Algorithm, a novel nature-inspired metaheuristic algorithm designed for complex optimization problems. Motivated by the unique social behaviors and cooperative hunting strategies of lions, LOA offers a population-based approach. The algorithm's effectiveness is demonstrated through its application to a three-area interconnected power system. This chapter presents a new design of load frequency controller for deregulated power systems with FACTS devices using Ant Lion Optimization algorithm. These FACTS devices are capable of controlling the network condition in a very fast manner and because of this reason, the usage of FACTS devices are more apt to improve the stability of power system. TCPS is a device that injects a variable series voltage to affect the power flow by modifying the phase angle. To stabilize the frequency oscillations, impacts of Thyristor Controlled Phase Shifter located in series with tie-line have been investigated. A time-domain objective function, optimized using LOA, tunes the parameters of a PI controller for Load Frequency Control. Simulation results across various loading conditions reveal that LOA-based controllers achieve superior performance compared to conventional PI controllers, particularly in settling times and other relevant performance indices.

1. Introduction

Load frequency control plays a vital role in power system operation, ensuring the reliable delivery of electricity while maintaining frequency stability. The primary objective of LFC is to minimize steady-state frequency deviations and effectively track load demands within interconnected multi-area power systems [1-3]. Traditionally, LFC research has employed linear feedback models and conventional controllers. However, these controllers often exhibit limitations, such as slow response times, inability to handle system nonlinearities, and difficulties in adapting to changing operating conditions [4-5]. Furthermore, small load changes in one area of an interconnected system can induce frequency and tie-line power fluctuations across all areas. Therefore, effective LFC requires a control system capable of restoring both area frequencies and tie-line powers to their set points or very close to them following a load disturbance [6]. Artificial intelligence-based control systems offer advantages over conventional integral controllers, including faster response and improved stability [7]. This research proposes a novel approach to LFC using the Lion Optimization Algorithm to optimize the parameters of a PI controller for a three-area interconnected power system [8]. The Integral of Time multiplied by Absolute Error criterion serves as the cost function for optimization, prioritizing the reduction of settling time and rapid damping of oscillations [9]. The proposed method utilizes Area Control Error feedback within each area to drive control actions, aiming to maintain zero ACE and consequently regulate frequency and tie-line power within prescribed limits [10]. This approach promises improved performance compared to conventional PI controllers, particularly in terms of control time and frequency deviation reduction during power system operation.

2. Three area interconnected power system

The system under study consists of three areas. Area one is a thermal non-reheat system, area two is a hydro system, and area three is photovoltaic (PV) system. The detailed designed model of three area power system for load frequency control is shown in Fig.1 [11]. The thermal plant has a single stage non-reheat steam turbine, and the hydro plant equipped with an electric governor.

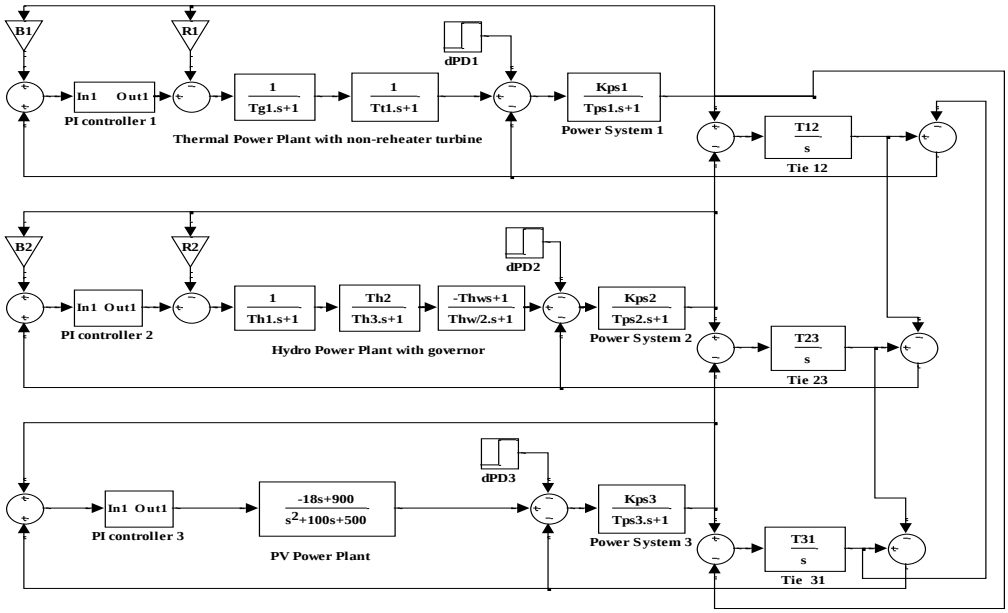

Fig. 1. A Three Area LFC power system model

2.1 System Modelling

The dynamic model of Load Frequency Control (LFC) for a two-area interconnected power system is presented in this section. Each area of the power system consists of speed governing system, turbine and generator as shown in Fig.1. Each area has three inputs and two outputs. The inputs are the controller input ΔPref, load disturbance ΔPD and tie-line power error ΔPTie [12]. The outputs are the generator frequency Δf and Area Control Error (ACE) given by equation

$$ACE = B \cdot \Delta f + \Delta P_{tie} \tag{1}$$

Where B is the frequency bias parameter

To simplicity the frequency-domain analyses, transfer functions are used to model each component of the area. Turbine is represented by the transfer function:

Transfer function of the governor is

$$G_g(s) = \frac{\Delta P_v(s)}{\Delta P_g(s)} = \frac{1}{T_{g1} \cdot s + 1} \tag{2}$$

Transfer function of the steam turbine is

$$G_t(s) = \frac{\Delta P_t(s)}{\Delta P_v(s)} = \frac{1}{T_t \cdot s + 1} \tag{3}$$

Transfer function of the generator is

$$G_p(s) = \frac{K_p \cdot s}{T_p \cdot s + 1} \tag{4}$$

Where $K_p = 1/D$ and $T_p = 2H/fD$

Transfer function of the hydraulic turbine is

$$G_{th}(s) = \frac{-Th_w \cdot s}{Th_w/2 \cdot s + 1} \quad (5)$$

The system under investigation consists of three area interconnected power system as shown in Fig.1. The system is widely used in literature is for the design and analysis of automatic load frequency control of interconnected areas. In Fig. 1, B_1 and B_2 are the frequency bias parameters; ACE_1, ACE_2 and ACE_3 are area control errors; u1, u2 and u3 are the control outputs form the controller; R_1 and R_2 are the governor speed regulation parameters in pu Hz; $T_{g1}$and T_{g2} are the speed governor time constants in sec; ΔP_{V1} and ΔP_{V2} are the change in governor valve positions (pu); ΔP_{g1} and ΔP_{g2} are the governor output command (pu); T_{t1} and T_{t2} are the turbine time constant in sec; ΔP_{t1} and ΔP_{t2} are the change in turbine output powers; dP_{D1}, dP_{D2} and dP_{D3} are the load demand changes; ΔPTie is the incremental change in tie line power (p.u); K_{PS1}, K_{PS2} and K_{PS3} are the power system gains; T_{PS1}, T_{PS2} and T_{PS3} are the power system time constant in sec; T_{12}, T_{23} and T_{31} are the synchronizing coefficient and Δf_1, Δf_2 and Δf_3 are the system frequency deviations in Hz.

2.2 Thyristor Controlled Phase Shifter (TCPS)

A Thyristor Controlled Phase Shifter (TCPS) is a successful power electronic device for the tie-line power flow control of an interconnected power system. TCPS is a device that changes the relative phase angle between the system voltages. The tie-line power flow can be regulated by controlling the phase angle to damp out the area frequency deviations and improve power system stability Parmar et al. (2012). The TCPS is connected in series with the tie-line as shown in Fig. 2 Shayeghi et al.(2009). During a sudden load variation in the power system, the TCPS swiftly starts to suppress the transient frequency deviations; then the governor systems takes over the control to compensate for the steady state frequency deviation Paramasivam & Chidambaram (2012). The transfer function blocks diagram of TCPS. Bhatt et al.(2010). Is shown in Fig. 3.

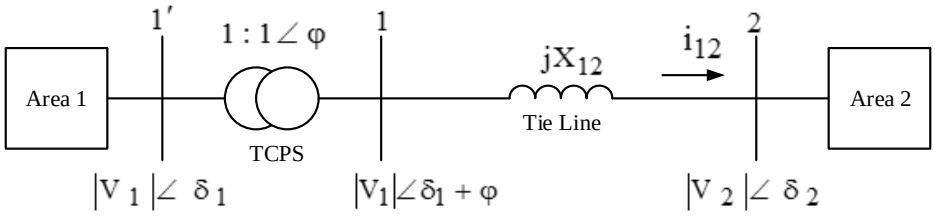

Fig. 2 Schematic diagram of TCPS connected in series with the ac tie-line

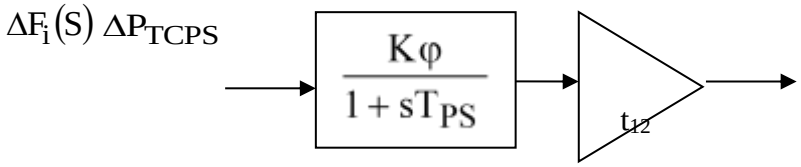

Fig. 3 Transfer function block diagram of TCPS

The interconnected tie-line power flow from area 1 to area 2 without considering TCPS can be expressed as

$$\Delta P_{tie12} = \frac{2\pi T_{12}}{s}\left[\Delta F_1 - \Delta F_2\right] \quad (6)$$

The TCPS is positioned in series with the tie-line as given in Fig. 6.1,

The complex power can be written as

$$P_{tie12} - jQ_{tie12} = |V_1| \angle -(\delta_1 - \varphi)\left(\frac{|V_2| - (\delta_1 - \varphi)|V_2| \angle \delta_2}{jX_{12}}\right) \quad (7)$$

Separating the real part and imaginary of tie-line power, the real part can be written as given below

$$\Delta P_{tie12} = \frac{|V_1||V_2|}{X_{12}} \sin(\delta_1 - \delta_2 + \varphi) \quad (8)$$

The tie-line power deviation is reduced as

$$\Delta P_{tie12} = T_{12}(\delta_1 - \delta_2) + T_{12}\Delta\varphi \quad (9)$$

We know that,

$$\Delta\delta_1 = 2\pi \int \Delta F_1 dt \quad \text{and} \quad \Delta\delta_2 = 2\pi \int \Delta F_2 dt$$

Therefore,

$$\Delta P_{tie12} = \left(\int \Delta F_1 dt - \int \Delta F_2 dt\right) + T_{12}\Delta\varphi \quad (10)$$

Taking Laplace transform of (6.5), we get

$$\Delta P_{tie12}(s) = \frac{2\pi T_{12}}{s}[\Delta F_1(s) - \Delta F_2(s)] + T_{12}\Delta\varphi(s) \quad (11)$$

The tie-line power flow in TCPS can be controlled by controlling the phase shifter angle$\Delta\varphi$. The phase shifter angle $\Delta\varphi$ (s) can be represented as

$$\Delta\varphi(s) = \frac{k\phi}{1 + sT_{ps}} \Delta Error_1(s) \quad (12)$$

In (6.7), T_{ps} is the time constant of TCPS unit and Kφ is the gain of TCPS unit. ΔF_1 is the input signal in the TCPS control logic.

$$\Delta P_{tie12}(s) = \frac{2\pi T_{12}}{s}[\Delta F_1(s) - \Delta F_2(s)] + T_{12}\frac{k\phi}{1 + sT_{ps}}\Delta F_1(s) \quad (13)$$

3. Design of PI for Load frequency control system

Notwithstanding the considerable advancements in control systems over the past two decades, the Proportional-Integral controller and its variations remain a mainstay in engineering practice. This enduring popularity stems from a combination of factors, including straightforward design and implementation, reliable operation, and a cost-effective balance between performance and expense [13]. Further contributing to their widespread use are the advantages of simplified dynamic modeling, reduced operator skill requirements, and minimized development effort all crucial considerations in practical engineering applications. The PI controller, as its name implies, comprises proportional and integral control modes. Proportional control reduces rise time but does not eliminate steady-state error, while integral control eliminates steady-state error but can negatively impact transient response characteristics [14]. The design of PI controller requires determination of the two parameters, Proportional gain (K_P) and Integral gain (K_I).

The error inputs to the controllers are the respective area control errors (ACE) are,

$$e_1(t) = ACE_1 = B_1\Delta f_1 + \Delta P_{tie12} \quad (14)$$

$$e_2(t) = ACE_2 = B_2\Delta f_2 + \Delta P_{tie23} \quad (15)$$

$$e_3(t) = ACE_3 = \Delta f_3 + \Delta P_{tie31} \quad (16)$$

The control inputs of the power system u1 and u2 are the outputs of the controllers. The control inputs are obtained as

$$u_1 = K_{P1}ACE_1 + K_{I1}\int ACE_1 \quad (17)$$

$$u_2 = K_{P2}ACE_2 + K_{I2}\int ACE_2 \quad (18)$$

$$u_3 = K_{P3}ACE_3 + K_{I3}\int ACE_3 \quad (19)$$

The design of a PI controller begins with defining an objective function that reflects the desired performance specifications and any system constraints. This objective function, used to tune the PI controller parameters, typically relies on a performance index that evaluates the overall closed-loop system response. Common time-domain output specifications considered include peak overshoot, rise time, settling time, and steady-state error. Frequently employed performance criteria for control design include the Integral of Time multiplied by Absolute Error, Integral of Squared Error, and Integral of Absolute Error [15].

The sum of time multiple absolute errors in ACE is considered as a performance index. Hence, J can be,

$$J = \sum_{i=1}^{N} \int_0^{tsim} t\left|ACE\right| \cdot dt \quad (20)$$

$$K_{Pi}^{\min} \le K_{Pi} \le K_{Pi}^{\max} \quad (21)$$

$$K_{Ii}^{\min} \le K_{Ii} \le K_{Ii}^{\max} \quad (22)$$

Where J is the objective function and $K_P^{\min}$, $K_I^{\min}$ and $K_P^{\max}$, $K_I^{\max}$ is the minimum and maximum value of the control parameters. One more important factor that affects the optimal solution more or less is the range for unknowns. The range of unknowns depends on the type of applications. For the very first execution of the program, a wider solution space can be given and after getting the solution one can shorten the solution space nearer to the values obtained in the previous iteration. To enhance the system response regarding the settling time and overshoots, it is necessary to modify the above equation. The design process can be formed as the following constrained optimization problem.

4. Lion Optimization algorithm (LOA)

Lions are the most socially inclined of all wild cat species which display high levels of cooperation and antagonism [16]. Lions are of particular interest because of their strong sexual dimorphism in both social behavior and appearance. The lion is a wild felid with two types of social organization: residents and nomads. Residents lives in groups, called pride [17]. A pride of lions typically includes about five females, their cubs of both sexes, and one or more than one adult males. Young males are excluded from their birth pride when they become sexually mature. As mention before, the second organiza- tional behavior is called nomads, who move about sporadi- cally, either in pairs or singularly. Pairs are more seen among related males who have been excluded from their maternal pride. Notice that a lion may switch lifestyles; residents may become nomads and vice versa [17].

Unlike all other cats, Lions typically hunt together with other members of their pride. Several lionesses work together and encircle the prey from different points and catch the victim with a fast attack. Coordinated group hunting brings a greater probability of success in lion hunts. The male lions and some lionesses usually stay and rest while waiting for the hunter lionesses to return from the hunt [18]. Lions do mate at any time of the year, and the females are polyestrous (when females not rearing their cubs are receptive) [19]. A lioness may mate with multiple

partners when she is in heat [20]. In nature, male and female lions mark their territory and elsewhere, which seems a good place with urine.

In this work, some characters of lions are mathematically modeled in order to design an optimization algorithm. In the proposed algorithm, Lion Optimization Algorithm (LOA), an initial population is formed by a set of randomly generated solutions called Lions.

Proposed algorithm

The LOA is a population-based meta-heuristic algorithm in which the first step is to randomly generate the population over the solution space. In this algorithm, every single solution is called ‘‘Lion”. In a Nvar dimensional optimization problem, a Lion is represented as follows:

$$Lion=[x_1, x_2, x_3, \ldots\ldots x_{Nvar}] \quad (23)$$

Cost (fitness value) of each lion is computed by evaluating the cost function, as:

$$\text{Fitness value of lion} = f[Lion] = f[x_1, x_2, x_3, \ldots\ldots x_{Nvar}] \quad (24)$$

In first step, N_{pop} solutions are generated randomly in search space. %N of generated solutions are randomly chosen as nomad lions. The rest of the population will be randomly divided into P prides. Every solution in this algorithm has a specific gender and remained constant during the optimization process. To emulating this fact, in each pride %S (%75–%90) of entire population formed in the last step are known as females and the rest as males. For nomad lions, this ratio is vice versa % (1S). Over the searching process every lion marks its best visited position. According to these marked positions, every pride's territory is formed. Therefore, for each pride, marked positions (best visited positions) by its members form that pride's territory.

Lion Optimization Algorithm pseudo code

1. *Generate random sample of Lions N_{pop} (N_{pop}) is the number of initial population).*
2. *Initiate prides and nomad lions: i. Randomly select %NNN (Percent of lions that are nomad) of the initial population as nomad lions. Partition remaining lions into PPP (PPP is the number of prides) prides randomly, and form each pride's territory. ii. In each pride, %SSS (Sex rate) of the entire population are known as females and the rest as males. This rate in nomad lions is inversed.*
3. *For each pride do: i. Some randomly selected female lions go hunting. ii. Each of the remaining female lions in the pride goes toward one of the best-selected positions from the territory. iii. In the pride, for each resident male, %RRR (Roaming percent) of the territory is randomly selected and checked. %MaM_aMa (Mating probability) of females in the pride mate with one or several resident males → New cubs become mature. iv. The weakest male is driven out from the pride and becomes nomad.*
4. *For nomad lions do: i. Nomad lions (both male and female) move randomly in search space. $\%M_a$ (Mating probability) of nomad females mate with one of the best nomad males → New cubs become mature. ii. Prides are randomly attacked by nomad males.*
5. *For each pride do: i. Some females with I rate (Immigrate rate) immigrate from the pride and become nomad.*
6. *Do: i. Based on their fitness value, each gender of the nomad lions is sorted. After that, the best females among them are selected and distributed to prides, filling empty places of migrated females. ii. With respect to the maximum permitted number of each gender, nomad lions with the least fitness values will be removed.*

The main steps of the LOA are summarized in the pseudo code shown above. To see how Lion Optimization Algorithm (LOA) is able to solve optimization problems, some points may be noted:

- In LOA, each solution has specific gender and each gender has its own strategy for searching. It assists Lion Optimization Algorithm (LOA) to look for optimal point by different strategies.
- The general aim in using several prides is that each pride focuses on a specific region and balance between exploration and exploitation. Its character of LOA increases capability of it to fit for the optimization on multi-modal problems.
- Nomad lions and their adaptive roaming assist Lion Optimization Algorithm (LOA) to search solution space randomly and escape from local optima.
- Personal best so far positions of lions can provide valuable and reliable information found so far by the population. The proposed pride's territory assists Lion Optimization Algorithm (LOA) to save the best solutions obtained so far over the course of iteration.
- In LOA, by mating, lions share information between genders while new cubs inherit character from both genders.
- Resident males roaming assist Lion Optimization Algorithm (LOA) to exploit information from their respective pride's neighbors that hold valuable knowledge. This procedure can be considered as a strong local search.
- The proposed encircling mechanism during hunting has two advantages; first of all, provides a circle-shaped neighbor- hood around the solutions and let opportunity for hunter to close to prey from different directions and second provides an opportunity for solutions to escape from local optima.

5. Result and Discussion

Load Frequency Control of three-area interconnected power system with FACTS device TCPS have been developed as shown in Fig.1. The proposed power system model is simulated in a separate program considering various load changes and time constants. The objective function is calculated and used in the optimization algorithm to evaluate the performance of the proposed LOA PI Controller. The simulated results are compared with Conventional PI Controller.

Case 1: Step Load Change in Area-1

A 10% step increase in demand was applied in Area-1, and the resulting system dynamic responses are presented in Fig. 4. Figs. 4(a) through 4(c) illustrate the frequency deviations in Area-1, Area-2, and Area-3, respectively. Figs. 4(d) through 4(f) depict the tie-line power deviations between Area-1 and Area-2, Area-2 and Area-3, and Area-3 and Area-1, respectively. Subsequently, a 20% step increase in demand was applied in Area-2 and a 10% step increase in Area-1. The corresponding system responses are shown in Fig. 5. Figs. 5(a) through 5(c) display the frequency deviations, while Figs. 5(d) through 5(f) present the tie-line power deviations, using the same area and tie-line designations as in Fig. 2. Analysis of the frequency and tie-line power deviations in the three-area power system demonstrates that the LOA-optimized PI controller yields optimal results and superior ISE, IAE, and ITAE values compared to the conventional PI controller.

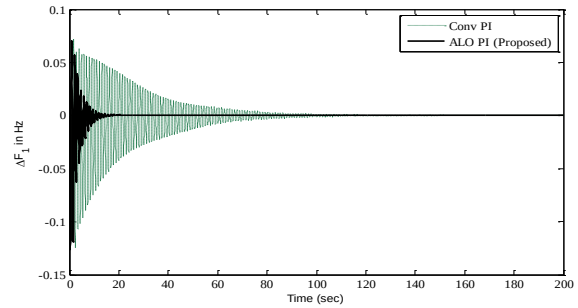

(a) Frequency deviation of area-1

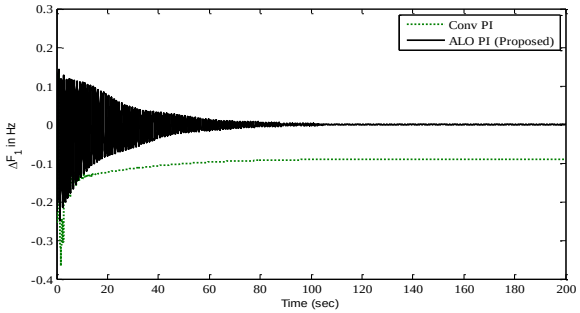

(a) Frequency deviation of area-1

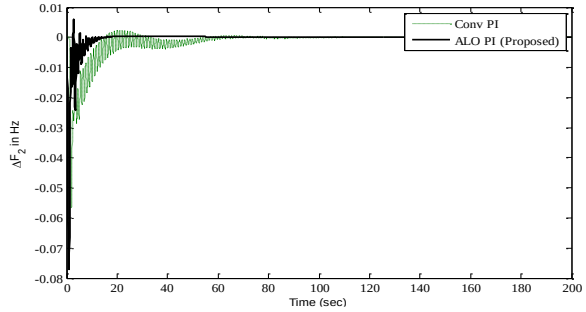

(b) Frequency deviation of area-2

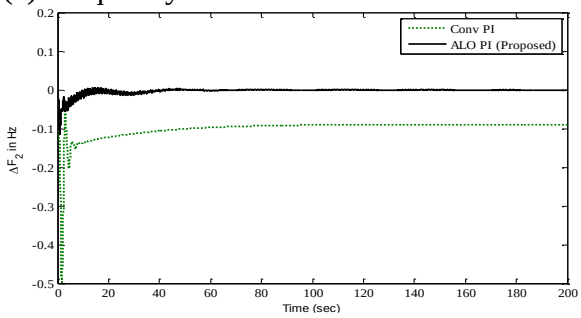

(b) Frequency deviation of area-2

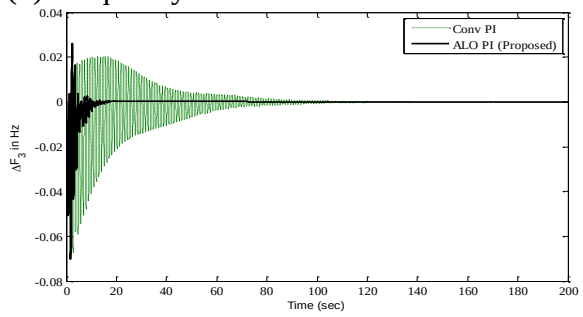

(c) Frequency deviation of area-3

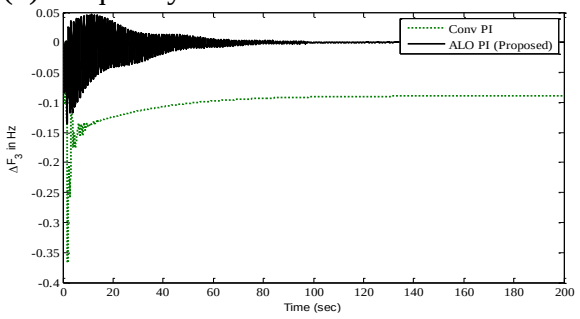

(c) Frequency deviation of area-3

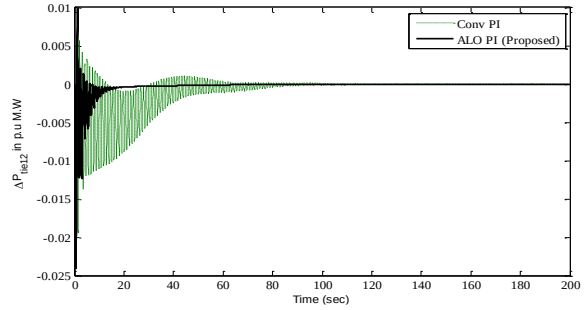

(d) Tie-line power deviation between area-12

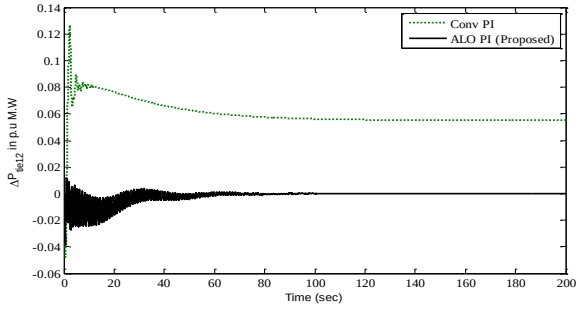

(d) Tie-line power deviation between area-12

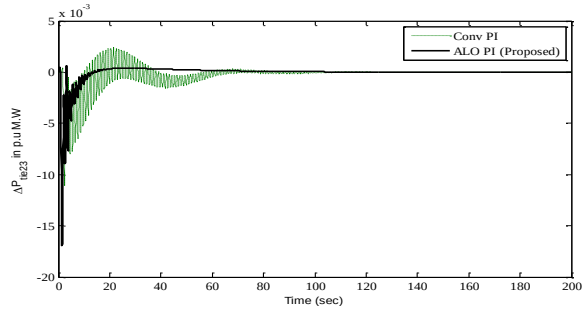

(e) Tie-line power deviation between area-23

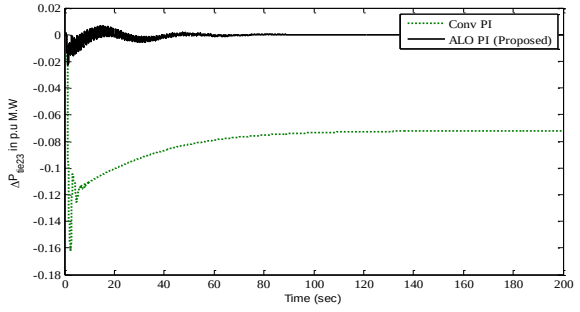

(e) Tie-line power deviation between area-23

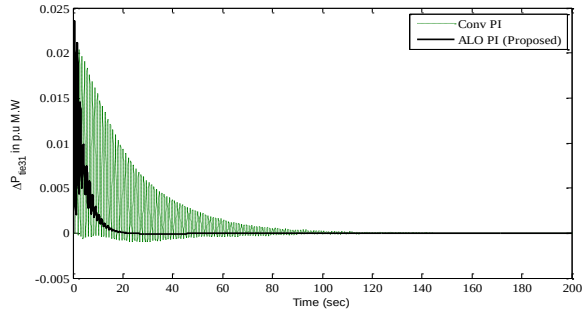

(f) Tie-line power deviation between area-31

Fig. 4 10% step increase in load demand in area-2 with TCPS

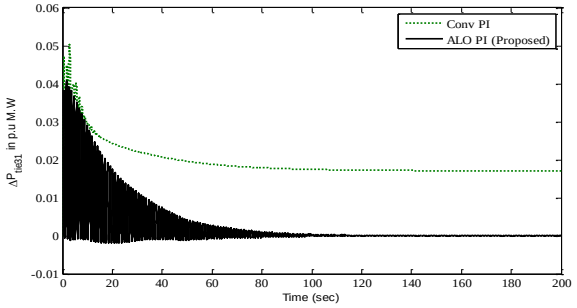

(f) Tie-line power deviation between area-31

Fig. 5 20% step increase in load demand in area-2 with TCPS

Case 2: Sensitivity Analysis with TCPS

Most of the cases the conventional PI controller responses were not settled properly, and their cost values are very high. To find the robustness of the power system, further, the operating load condition and time conditions of a speed governor, steam turbine, tie-line power, hydro turbine and hydro governor are varied from their nominal values in the range of +25% and -25%. The change in operating load condition affects the power system parameters KPS and TPS. The change in tie-line power is simulated by changing the synchronizing coefficient T12.

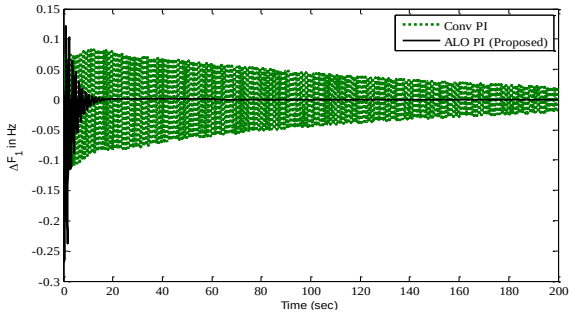

(a) Frequency deviation of area-1

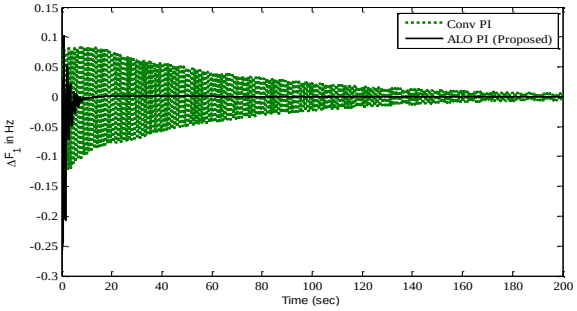

(a) Frequency deviation of area-1

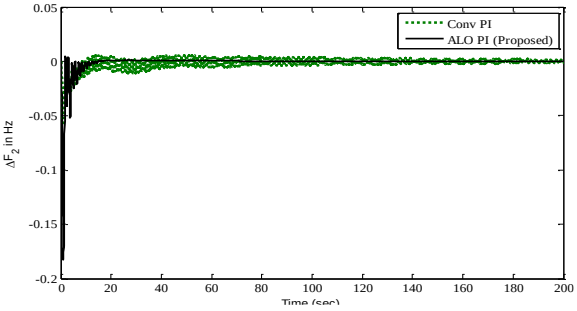

(b) Frequency deviation of area-2

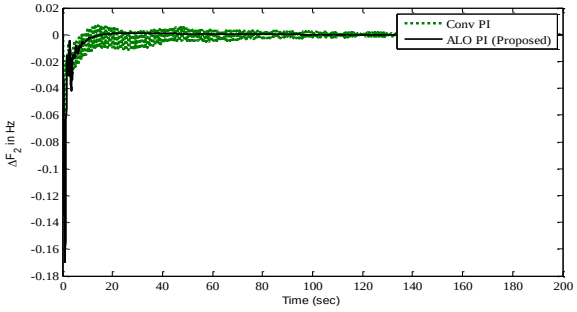

(b) Frequency deviation of area-2

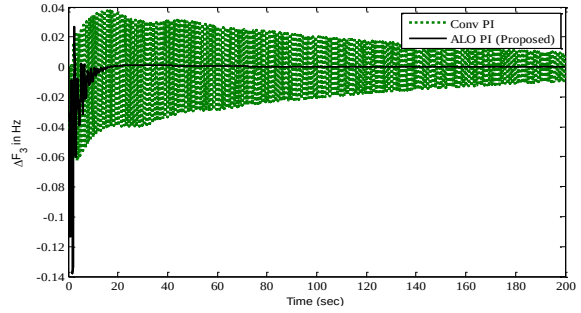

(c) Frequency deviation of area-3

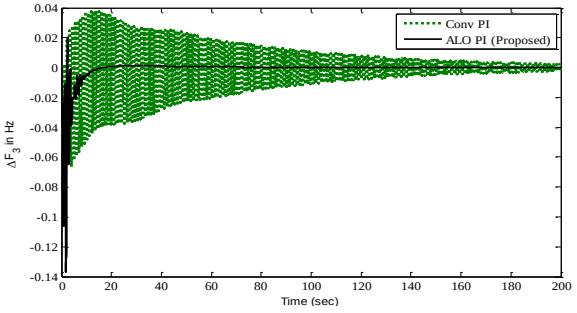

(c) Frequency deviation of area-3

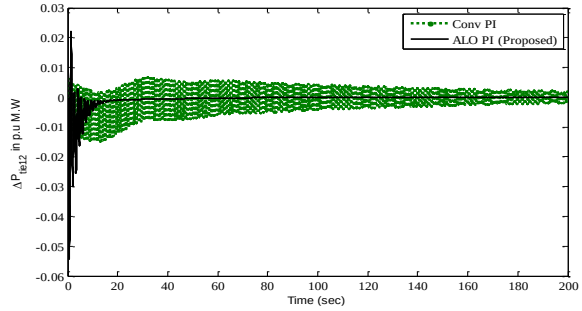

(d) Tie-line power deviation between area-12

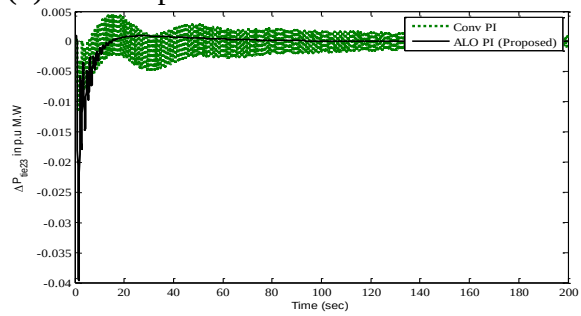

(e) Tie-line power deviation between area-23

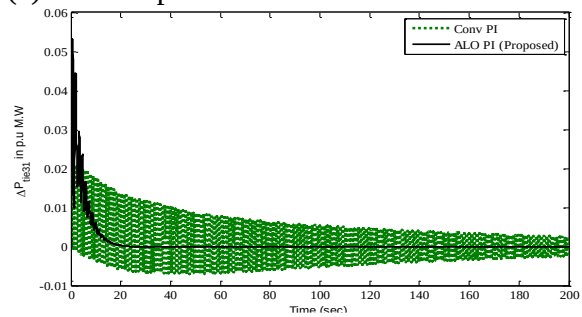

(f) Tie-line power deviation between area-31

Fig. 6 +25% change in T_G with TCPS

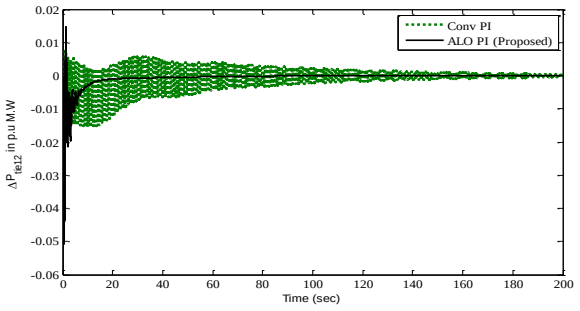

(d) Tie-line power deviation between area-12

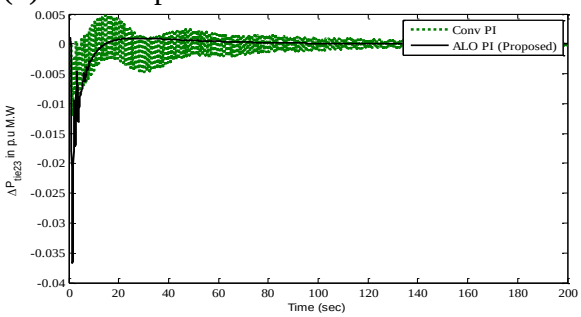

(e) Tie-line power deviation between area-23

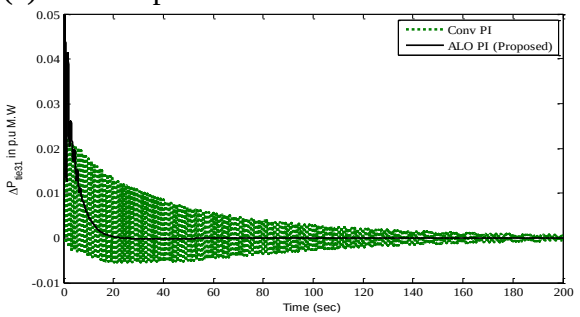

(f) Tie-line power deviation between area-31

Fig. 7 +25% change in T_T with TCPS

Figs. 6(a) to 6(c) show the frequency deviation of area-1, area-2 and area-3 and Figs. 6(d) to 6(f) show the tie-line power deviation between area-12, area-23 and area-31 for steam governor (T_G) with 25% of increment. From the results of speed governor load variation; it is observed that the LOA PI controller generated a better response with minimum cost values compared to conventional PI controller. Figs. 7(a) to 7(c) show the frequency deviation of area-1, area-2 and area-3 and Figs. 7(d) to 7(f) show the tie-line power deviation between area-12, area-23 and area-31 for steam turbine (T_T) with 25% of increment. From the results of steam turbine (T_T) load variation; it is observed that the LOA PI controller generated a better response with minimum cost values compared to conventional PI controller.

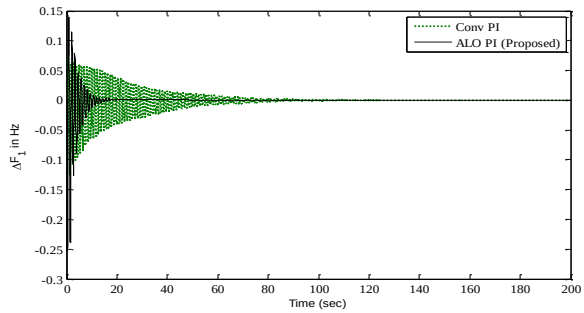

(a) Frequency deviation of area-1

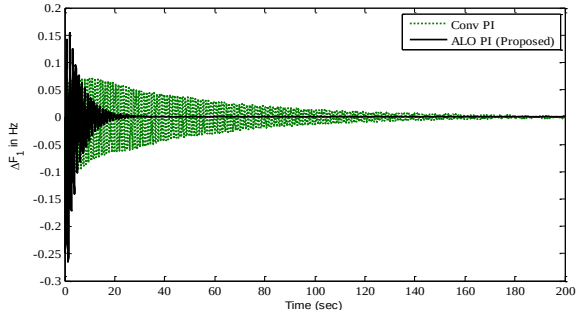

(a) Frequency deviation of area-1

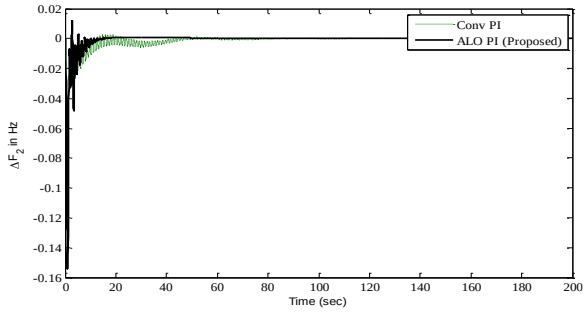

(b) Frequency deviation of area-2

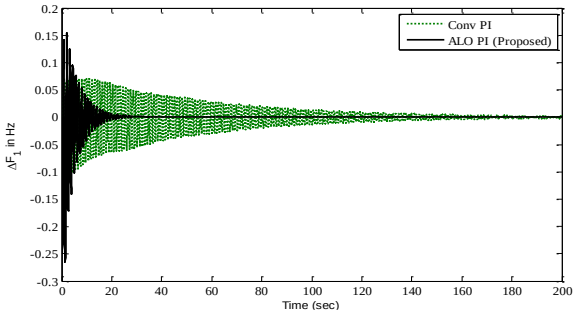

(b) Frequency deviation of area-2

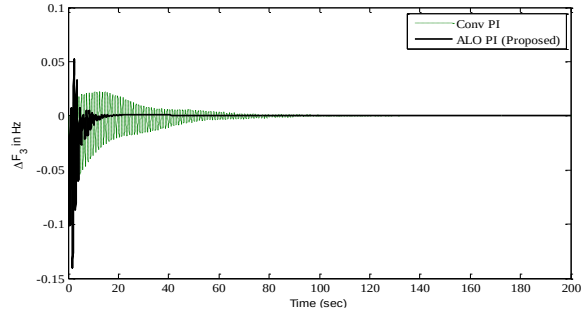

(c) Frequency deviation of area-3

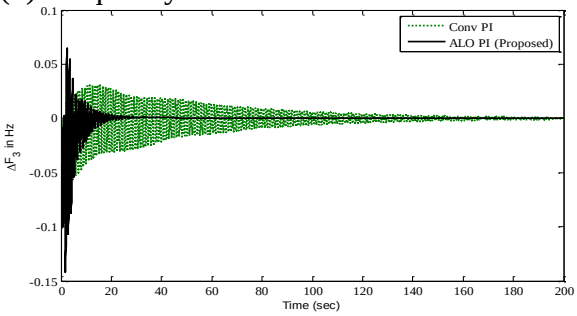

(c) Frequency deviation of area-3

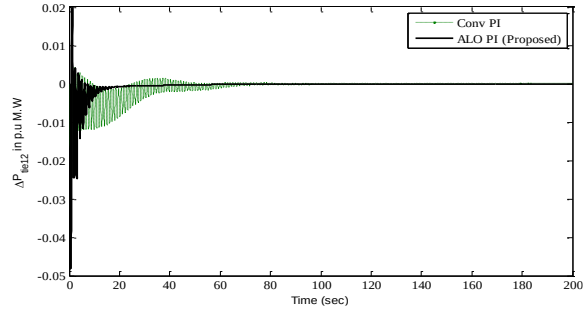

(d) Tie-line power deviation between area-12

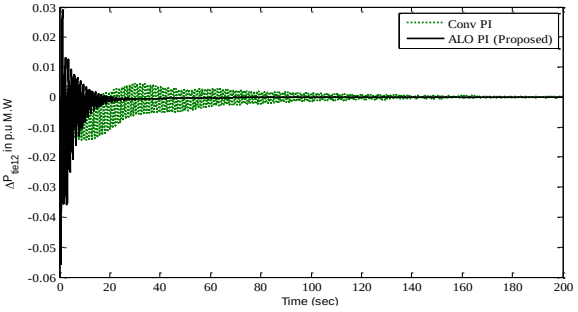

(d) Tie-line power deviation between area-12

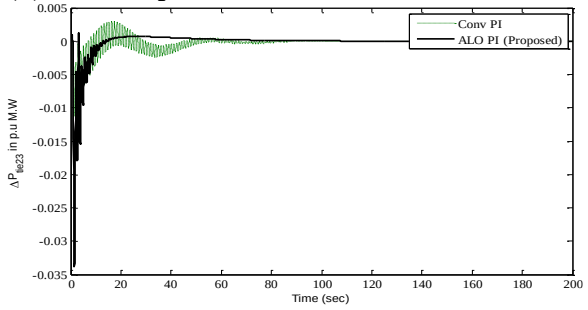

(e) Tie-line power deviation between area-23

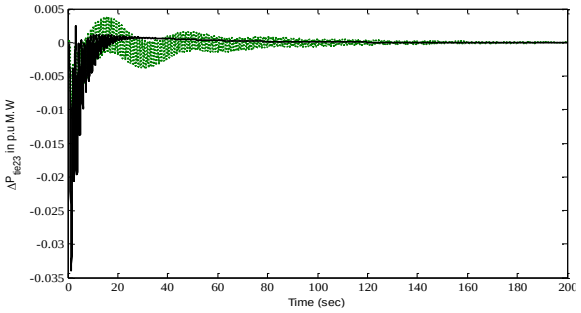

(e) Tie-line power deviation between area-23

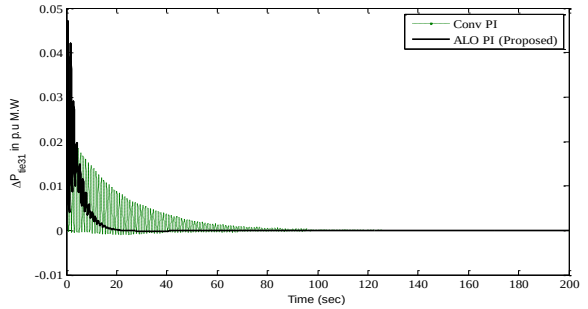

(f) Tie-line power deviation between area-31

Fig. 8 +25% change in T_{H1} with TCPS

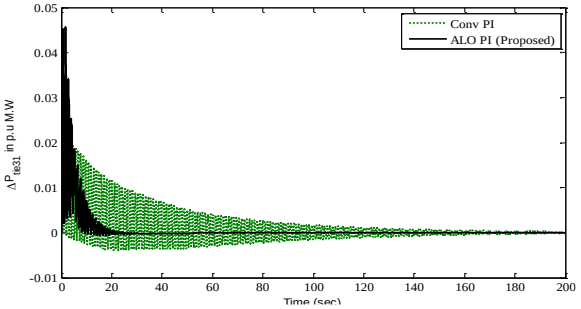

(f) Tie-line power deviation between area-31

Fig. 9 +25% change in T_{12} with TCPS

Figs. 8(a) to 8(f) show the frequency deviation and tie-line power deviation of three-area interconnected power system for speed governor (Th1) with 25% increment. From the results; it is observed that the LOA PI controller produced a better response with minimum cost values compared to conventional PI controller. Figs. 9(a) to 8(f) show the frequency deviation and tie-

line power deviation of three-area interconnected power system for tie-line power (T_{12}) with 25% increment. From the results; it is observed that the LOA PI controller produced a better response with minimum cost values compared to conventional PI controller. The results obtained are depicted in Tables 1 and 2. Table 1 compares the performance of two controllers, Conventional PI (Conv PI) and LOA PI, under specific load change scenarios in terms of performance indices and settling times. The scenarios include a 10% load change in area 1 and a combined 20% load change in area 2 with 10% in area 1. The performance indices, including the Integral of Squared Error (ISE), Integral of Absolute Error (IAE), and Integral of Time-weighted Absolute Error (ITAE), reveal that the LOA PI controller significantly outperforms the Conv PI controller in both cases, with much lower values, indicating more efficient error handling. Furthermore, LOA PI stabilizes the system much faster, with settling times ranging between 10–21 seconds, compared to the Conv PI, which exhibits longer or unreported settling times. These results demonstrate the robustness and superior control performance of the LOA PI controller in managing system stability and minimizing error under varying load conditions.

Table 1 Simulated response of LFC Three-area Interconnected Power System for case 1 with TCPS

Parameter	% Change	Controller	Performance Index			Settling Time (Ts)		
			ISE	IAE	ITAE	ΔF_1	ΔF_2	ΔF_3
Case 1	10% load	687.2543	2.4023e+	4.8761e+	113.30	94.29	110.9	687.2543
		219.1000	2.6740e^3	1.3483e^4	27.1	26.92	32.27	219.1000
	20% load change in	2.5796e+	4.5427e+	8.7791e+	-	-	-	2.5796e+
		1.3273e+003	1.3760e+004	2.9543e+004	84.99	43.7	89.32	1.3273e+003

Table 2 Sensitivity analysis for Case 2 with TCPS

Parameter Variation	% Change	Controller	Performance Index			Settling Time (Ts) in sec		
			ISE	IAE	ITAE	ΔF_1	ΔF_2	ΔF_3
Case 2	+25% in T_G	Conv PI	2.4170e+003	6.5980e+004	3.2888e+06	140.6	79.9	130.7
		LOA PI	678.0747	1.8211e^3	7.4734e^5	21.28	17.9	18.91
	+25% in T_T	Conv PI	1.8112e+003	5.1996e+004	2.0302e+006	150.2	144.2	160.1
		LOA PI	521.9896	8.4412e^3	6.8465e^4	18.91	15.83	16.98
	+25% in T_{12}	Conv PI	1.2332e+003	4.0432e+004	1.3645e+006	102.8	130	135.1
		LOA PI	842.1020	1.2097e^4	8.7903e^4	30.56	30.39	35.47
	+25% in T_{H1}	Conv PI	640.3085	2.2469e+04	4.3259e+05	113.4	85.77	116.8
		LOA PI	198.2386	8.6468e^3	5.4901e^4	21.62	19.06	22.86

The table compares the performance of Conventional PI (Conv PI) and LOA PI controllers under different parameter variation scenarios, specifically a 25% increase in T_G (governor time constant), T_T (turbine time constant), T_{12} (tie line), and T_{H1} (reheat time constant). Performance is evaluated using three indices: Integral of Squared Error (ISE), Integral of Absolute Error (IAE), and Integral of Time-weighted Absolute Error (ITAE), as well as the settling time (T_s) for frequency deviations (ΔF_1, ΔF_2, and ΔF_3). Across all scenarios, the LOA

PI controller demonstrates superior performance, with significantly lower ISE, IAE, and ITAE values, indicating better error handling, and shorter settling times, ranging from 17 to 68 seconds. In contrast, the Conv PI controller exhibits higher performance indices, reflecting poorer efficiency, and in many cases, does not report settling times. These results highlight the robustness and effectiveness of the LOA PI controller in maintaining system stability under parameter variations.

6. Conclusion

The simulation results show the effectiveness of TCPS in suppressing inter-area frequency deviations and tie line power deviations in LFC of proposed three-area interconnected power system. The effectiveness of optimal PI controller obtained using LOA algorithm with TCPS has also been proved. The LOA tuned controller along with TCPS enhances the performance of three-area interconnected power system to a well-accepted level with optimal performance. TCPS provides more flexibility in power system operation and control. Each device has its unique advantage.

Appendix A

Nominal parameters of the three area system investigated are [12]:

P_R = 2000 MW (rating), P_L = 1000 MW (nominal loading); f = 60 Hz, B_1=B_2 = 0.425 p.u. MW/Hz; R_1= R_2 = 2.4 Hz/p.u.; T_{g1} = 0.08 s; T_{t1} = 0.3 s; K_{PS1} = K_{PS2} = K_{PS3} =120 Hz/p.u. MW; T_{PS1} = T_{PS2} =T_{PS3} = 20 s; T_{12} = T_{23} = T_{31} = 0.545 pu; T_{h1} = 48.7s; T_{h2} = 0.513s; T_{h3} = 10s; T_{hw} = 1.0s.

References

1. Parmar, K. P. S., Majhi, S., & Kothari, D. P. (2013). LFC of an interconnected power system with multi-source power generation in deregulated power environment. In International Journal of Electrical Power & Energy Systems (Vol. 57, p. 277). Elsevier BV. https://doi.org/10.1016/j.ijepes.2013.11.058
2. P. Kundur, Power System Stability and control, TMH, 8th reprint 2009.
3. O.I. Elgerd, Electric energy systems theory. An introduction. New Delhi: Tata McGraw-Hill; 1983.
4. Shankar, R., Pradhan, S. R., Chatterjee, K., & Mandal, R. (2017). A comprehensive state of the art literature survey on LFC mechanism for power system. In Renewable and Sustainable Energy Reviews (Vol. 76, p. 1185). Elsevier BV. https://doi.org/10.1016/j.rser.2017.02.064
5. Obuz, S., Ayar, M., Trevizan, R. D., Ruben, C., & Bretas, A. S. (2019). Renewable and energy storage resources for enhancing transient stability margins: A PDE-based nonlinear control strategy. In International Journal of Electrical Power & Energy Systems (Vol. 116, p. 105510). Elsevier BV. https://doi.org/10.1016/j.ijepes.2019.105510
6. Wang, J. K., & Peng, C. (2017). Analysis of Time Delay Attacks against Power Grid Stability (p. 67). https://doi.org/10.1145/3055386.3055392
7. Yousefian, R., & Kamalasadan, S. (2017). A Review of Neural Network Based Machine Learning Approaches for Rotor Angle Stability Control [Review of A Review of Neural Network Based Machine Learning Approaches for Rotor Angle Stability Control]. arXiv (Cornell University). Cornell University. https://doi.org/10.48550/arxiv.1701.01214
8. Watson, J. D., Ojo, Y., Laib, K., & Lestas, I. (2020). A scalable control design for grid-forming inverters in microgrids. In arXiv (Cornell University). Cornell University. https://doi.org/10.48550/arxiv.2012.11556
9. Sharma, D., & Yadav, N. K. (2019). Lion Algorithm with Levy Update: Load frequency controlling scheme for two-area interconnected multi-source power system. In

Transactions of the Institute of Measurement and Control (Vol. 41, Issue 14, p. 4084). SAGE Publishing. https://doi.org/10.1177/0142331219848033
10. Dong, L., Zhang, Y., & Gao, Z. (2012). A robust decentralized load frequency controller for interconnected power systems. In ISA Transactions (Vol. 51, Issue 3, p. 410). Elsevier BV.
11. Salpakari, J., Mikkola, J., & Lund, P. D. (2016). Improved flexibility with large-scale variable renewable power in cities through optimal demand side management and power-to-heat conversion. In Energy Conversion and Management (Vol. 126, p. 649). Elsevier BV.
12. Liao, W., Bak-Jensen, B., Pillai, J. R., Wang, Y., & Wang, Y. (2021). A Review of Graph Neural Networks and Their Applications in Power Systems [Review of A Review of Graph Neural Networks and Their Applications in Power Systems]. arXiv (Cornell University). Cornell University.
13. Muppoori, N. (2020). Automatic Generation Control of Two Area Power System with Hybrid Control Technique. In International Journal of Engineering Research and (Issue 9). International Research Publication House. https://doi.org/10.17577/ijertv9is090377
14. Vilanova, R., & Visioli, A. (2017). The Proportional-Integral-Derivative (PID) Controller. In Wiley Encyclopedia of Electrical and Electronics Engineering (p. 1).
15. Jiao, X., Li, G., & Wang, H. (2018). Adaptive finite time servo control for automotive electronic throttle with experimental analysis. In Mechatronics (Vol. 53, p. 192). Elsevier BV.
16. Mccomb, K, et al. Female lions can identify potentially infanticidal males from their roars. Proc. R. Soc. Lond. Ser B: Biol. Sci. 1993;252 (1333)59–64.
17. Schaller GB. The Serengeti lion: a study of predator–prey relations. Wildlife behavior and ecology series. Chicago, Illinois, USA: University of Chicago Press; 1972.
18. Scheel D, Packer C. Group hunting behaviour of lions: a search for cooperation. Anim. Behav. 1991;41(4)697–709.
19. Wilkins J. How Many Species Concepts are tHERE. London: The Guardian; 2010.
20. S.B., Hrdy, 7 Empathy, polyandry, and the myth of the coy female, Conceptual Issues in Evolutionary Biology, 2006: p. 131.